

## Small-angle x-ray scattering study of phase separation in amorphous alloys during heating with use of synchrotron radiation

A. R. Yavari

*Laboratoire de Thermodynamique Physico-Chimie Métallurgiques, Institut National Polytechnique de Grenoble, Boîte Postale No. 75, F-38042 Saint-Martin-d'Herès, France*

K. Osamura and H. Okuda

*Department of Metallurgy, Kyoto University, Sakyo-ku, Kyoto 606, Japan*

Y. Amemia

*Photon Factory, National Laboratory for High Energy Physics (K.E.K.), Tsukuba-gun, Ibaraki 305, Japan*  
(Received 9 February 1987; revised manuscript received 12 November 1987)

Some recent reports suggest that amorphous  $\text{Pd}_{46}\text{Ni}_{36}\text{P}_{18}$  and  $\text{Cu}_{50}\text{Zr}_{50}$  alloys phase separate during heating at temperatures 50–200 K below their crystallization temperatures. We have therefore obtained improved small-angle x-ray scattering (SAXS) measurements during heating of these alloys using a new experimental setup. The experimental improvements included in-the-beam heating using the very-high-intensity x-ray radiation available at the Synchrotron Radiation Laboratory, K.E.K., the use of Joule self-heating of the samples, which is made possible by the high resistivity of the amorphous phase and the use of regularly shaped, constant thickness amorphous tapes obtained by planar flow casting. No evidence of phase separation during heating prior to crystallization was obtained in glassy  $\text{Pd}_{46}\text{Ni}_{36}\text{P}_{18}$  and  $\text{Cu}_{50}\text{Zr}_{50}$  alloys.

### I. INTRODUCTION

Metallic glasses which are metastable, crystallize when reheated near or above their temperatures of glass transition ( $T_g$ ) or crystallization ( $T_{\text{cryst}}$ ). Easy glass-forming alloys prepared by liquid quenching often consist of elements with strongly attractive interactions and large differences in atomic diameters. In many of these systems particular fractions of constituent atoms result in enhanced stability of the liquid state as evidenced by the occurrence of deep eutectics while other compositions in the same alloy systems produce very stable intermetallic crystalline phases with high melting temperature  $T_m$ .

When the glassy alloy is reheated near or above the temperatures of glass transition ( $T_g$ ) or crystallization ( $T_{\text{cryst}}$ ) the stable intermetallic phases form by nucleation and growth. In cases where the crystalline phase is of a different composition than the glassy phase, nucleation of the small crystallites requires important local compositional fluctuations in the glass. If such chemical fluctuations occur without development of long-range order, they result in a phase separated glass but thermodynamic and kinetic factors are such that the development of these zones of compositional fluctuations which require atomic mobility on the scale of their dimensions will usually also result in crystallization.

While Bragg peaks are absent from the diffraction spectra of amorphous alloys, the angular position of the principal halo in the diffraction pattern is related to the average diameter or interatomic distance  $d$  in each alloy. In particular the angular position  $2\theta_m$  of the maximum of the principal amorphous halo is proportional to

$\sin^{-1}(\lambda/2d)$  where  $\lambda$  is the radiation wave length. Since in most easy glass-forming alloys the atomic diameters of the major elemental constituents are very different, the shape and position of the diffraction halo should be modified if phase separation results in the formation of zones with significant differences in composition. The angular distribution of the diffracted intensity and the total structure factor may vary with composition in such a way, that if compositional variations are slight, a separation of contributions from different zones may not be possible. However, if for example two types of zones with very different compositions appear, they should result in diffraction spectra with two major amorphous halos with well resolved maxima at two different angular positions  $\theta_m$ . This has indeed been observed in several amorphous alloys<sup>1–3</sup> but only in the *as-quenched* state where phase separation has occurred during rapid quenching and at temperatures  $T > T_g$ .

Chou and Turnbull<sup>4</sup> first performed small-angle x-ray scattering (SAXS) experiments to study phase separation in glassy Pd-Au-Si and reported a phase separation at temperatures just a few degrees below crystallization. More recently several authors have attributed evolutions of various properties of amorphous alloys during relaxation annealing at temperatures well below  $T_g$  and  $T_{\text{cryst}}$  to phase-separation phenomena. Walter *et al.*, using SAXS (Ref. 5) and Auger-electron spectroscopy (AES) (Ref. 6) attributed the thermal embrittlement of glassy Fe-Ni-P-B-type alloys to the development of phase separation on a scale of tens of angstroms during relaxation annealing some 200 K below  $T_g$ .

We have studied structural evolution during annealing

of amorphous Fe-Ni-P alloys using small-angle neutron scattering (SANS) during in-the-beam heating<sup>7</sup> and using SAXS (Ref. 8) and Auger-electron spectroscopy<sup>9</sup> and found no such phenomena intervening during heat treatments similar to those of Walter *et al.*<sup>5,6</sup> for an Fe-Ni-P-B glassy alloy. Schultz *et al.*<sup>10</sup> studied the evolution of the resistivity and the shape of the diffraction halo of a glassy  $\text{Cu}_{50}\text{Zr}_{50}$  sample during different heat treatments. From these observations and transmission electron microscopy (TEM) images, they concluded that the glass phase separates on a scale of  $\approx 100 \text{ \AA}$  near 623 K while it crystallizes after some  $10^4$  sec at 658 K. Schluckebier and Predel<sup>11</sup> interpreted the occurrence of two glass-transition temperatures in the differential scanning calorimetry (DSC) spectra of some annealed Pd-Ni-P alloys with P content less than 20 at. % in terms of a phase separation into glassy zones with different compositions and glass transitions. In Fe-Ni-B glasses, Piller and Haasen<sup>12</sup> found that embrittlement during relaxation annealing at about 100 K below  $T_g$  correlated with the formation of zones some 10 to 50  $\text{\AA}$  in size rich and poor in boron as detected by atom-probe depth profiles and field ion microscopy (FIM).

The phase decomposition of crystalline metastable structures such as quenched Al-Zn alloys has been well documented in particular using conventional SAXS (Ref. 13) and more recently by real time SAXS measurements during phase decomposition using high-intensity light from a powerful synchrotron source.<sup>14</sup> The SAXS signal appearing during crystallization and phase separation in amorphous alloys is significantly weaker than in the case of phase decomposition of Al-Zn-type supersaturated crystalline alloys and very high-intensity beams are necessary for real-time measurements. Weak SAXS signals can be seriously affected by experimental problems when the samples are repeatedly furnace annealed, cooled and transferred to the x-ray camera for each measurement or if different samples are used for different heat treatments. The difficulties are further magnified by important local variations in the thickness of samples prepared by melt spinning mainly due to deep cavities caused by gas bubbles trapped between the ribbon and the substrate. These difficulties are reduced when very regular tapes are prepared by planar flow casting (PFC) under optimum conditions<sup>15,16</sup> and when the glass-forming tendency of the alloy allows amorphous thicknesses greater than 30  $\mu\text{m}$  which can then be reduced by polishing thus removing most defects from each face.

In the SAXS measurements reported here, we have attempted to minimize experimental difficulties by using a new experimental arrangement for SAXS measurements on wide and regular glassy alloy tapes annealed *in-situ* by direct Joule heating while exposed to high intensity x-radiation from the K.E.K. synchrotron radiation source. In this paper we report the first such SAXS measurements on amorphous  $\text{Cu}_{50}\text{Zr}_{50}$  and  $\text{Pd}_{46}\text{Ni}_{36}\text{P}_{18}$  tapes. Based on the previous studies already mentioned, each of these glassy alloys was expected to phase separate during heating well below crystallization at  $T_x$ . The Fe-Ni-B system was not retained because our previous analysis

had indicated that the SAXS signal would be too low for this alloy.<sup>17</sup>

## II. EXPERIMENTAL PROCEDURE

1 cm wide and 35  $\mu\text{m}$  thick  $\text{Cu}_{50}\text{Zr}_{50}$  and 3 cm wide and 100  $\mu\text{m}$  thick  $\text{Pd}_{46}\text{Ni}_{36}\text{P}_{18}$  (also referred as CuZr and Pd-Ni-P) were prepared by planar flow casting at the Laboratoire de Thermodynamique Physico-Chimie Métallurgique (LTPCM). Absence of crystallinity in the ribbons was checked by x-ray diffraction on both faces of the ribbons. The tapes were mechanically polished to reduce thicknesses to between 15 and 20  $\mu\text{m}$  both to facilitate transmission of x-rays and to remove oxide layers and cavities due to trapped gas bubbles. The SAXS experiments were performed at the synchrotron radiation laboratory, K.E.K., in Tsukuba, Japan. The very high-intensity x-ray beam was monochromatized to obtain a radiation wavelength of 1.54  $\text{\AA}$  similar to that of Cu  $K\alpha$ . In-the-beam heating of the amorphous tapes was done by Joule self-heating in a newly developed apparatus.<sup>18</sup> This apparatus is a vacuum tight stainless-steel furnace with two x-rays windows made of Kapton sheets (a Dupont product) and equipped with thermocouple and current leads. The microthermocouples embedded in the tapes are connected to a millivolt meter recorder. The current leads inside the furnace are hooked to copper plates on which the sample tape ends are clamped. On the outside, they are connected to a constant current source. The sample is self-heated by the power  $P=I^2R_0$  generated in the sample of resistance  $R_0$  when a constant current  $I$  is supplied. The high resistivity of amorphous alloys makes self-heating particularly attractive with these materials. The sample temperature response time to current changes is extremely short thus allowing well controlled thermal cycling controlled by the supplied current intensity. Heating rates of the order of 100 K/s are possible when  $I$  is increased rapidly but in this experiment rates of a few degrees per minute were chosen to allow acquisition of appropriate real-time scattering signals with the structural evolution of the sample during heating. It was found that the high-intensity beam allowed proper statistics for a counting time of about 2 min per frame. Heating rates of 2 to 3 K/min thus provided one spectrum (frame) for every  $\Delta T < 10 \text{ K}$  during heating [see (18) for more details]. Such heating rates are also in the range accessible on most DSC calorimeters and the SAXS changes with temperature can thus be compared to DSC curves if necessary.

A camera length of 2 m was used for the experiment. The scattering intensity  $I(Q, T)$  was obtained in a wave vector range of  $0.014 \leq Q \leq 0.258 \text{ \AA}^{-1}$ . Transmission intensities were measured repeatedly for the apparatus without any sample and with each sample. It was found that the background intensity  $I_0$  (apparatus without any sample and filled with He gas) was very weak compared to sample scattering intensity  $I(Q)$ .

The sample scattering intensity may be corrected for background scattering in the usual way with

$$I(Q) = I_{s+b}(Q) - T_s(I_{s+b}^{\text{in}}/I_b^{\text{in}})I_b(Q), \quad (1)$$

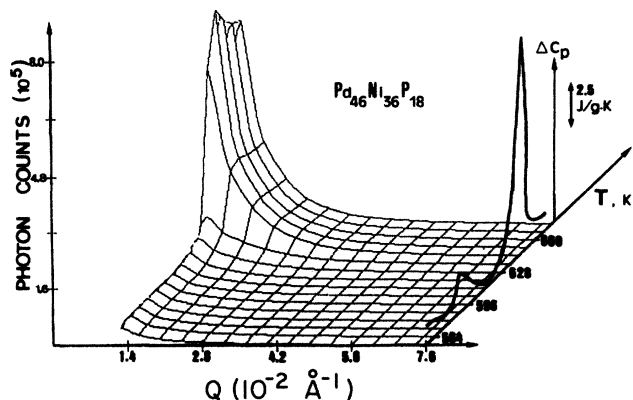


FIG. 1. Small-angle scattering intensity  $I(Q, T)$  in amorphous  $\text{Pd}_{46}\text{Ni}_{36}\text{P}_{18}$  as a function of temperature  $T$  and wave vector  $Q$  during heating at 2 K/min. Also shown is DSC thermogram for same alloy heated at the same rate.

where  $I_{s+b}$  and  $I_b$  are incident photon counts for sample plus background and background alone, respectively, each integrated over the measuring time and  $T_s$  is the sample transmission coefficient.

$I(Q)$  of Eq. (1) is coherent plus incoherent scattering from the sample and the latter includes fluorescence radiation  $I_f$  from the sample. For the wavelength of the experiment,  $I_f$  is negligible for Cu-Zr and Pd-Ni-P. Concerning corrections for background  $I_b(Q)$  due to apparatus (with gas) without any sample, it turns out that this contribution is very weak at low  $Q$  in our experiment such that for an overview of the results, it is sufficient to plot  $I_{s+b}(Q)$  instead of  $I(Q)$ . Figure 1 shows  $I_{s+b}(Q)$  curves for Pd-Ni-P alloy. The product  $T_s(I_{s+b}/I_b)I_b(Q)$  is too low to be visible. Figure 2 shows such curves for amorphous Cu-Zr on which we have also shown the product  $T_s(I_{s+b}/I_b)I_b(Q)$  for comparison. The suitable weak background scattering is partly due to the use of Kapton windows for our furnace.

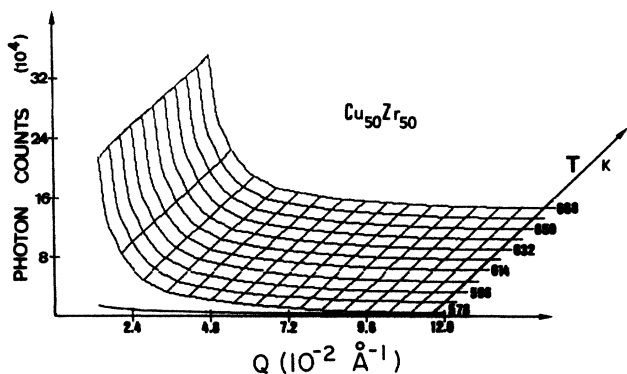


FIG. 2.  $I(Q, T)$  in amorphous  $\text{Cu}_{50}\text{Zr}_{50}$  during heating between 578 and 668 K at rate of 3 K/min.

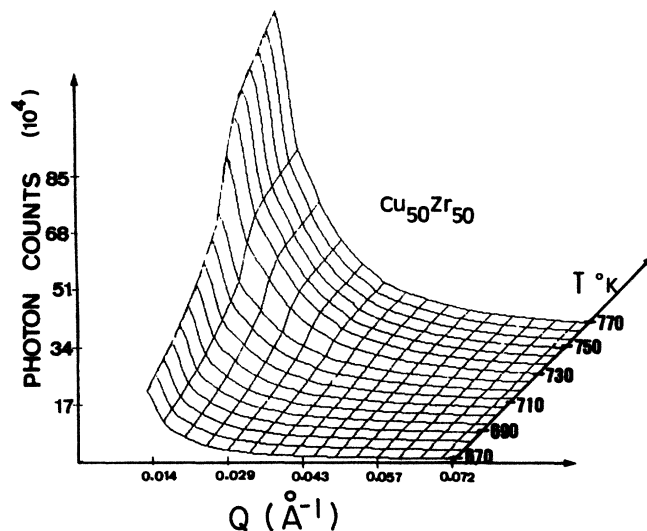


FIG. 3.  $I(Q, T)$  in amorphous  $\text{Cu}_{50}\text{Zr}_{50}$  during heating between 670 and 770 K at a rate of 3 K/min. Crystallization begins near 690 K.

### III. EXPERIMENTAL RESULTS

#### A. The isochronal heating of amorphous $\text{Pd}_{46}\text{Ni}_{36}\text{P}_{18}$

Figure 1 shows small angle scattering  $I(Q, T)$  measured during *in-situ* isochronal heating of the amorphous  $\text{Pd}_{46}\text{Ni}_{36}\text{P}_{18}$  foil in the temperature range  $553 \leq T \leq 673$  K and the wave-vector range  $0.014 \leq Q \leq 0.07 \text{ \AA}^{-1}$  with a heating rate of 2 K/min. Also shown in the figure is a DSC thermogram of the same foil heated at the same rate. DSC measurements have shown that if the sample is heated up to the end of the first (smaller) exotherm or to about 610 K, cooled and then reheated, two glass-transition temperatures can then be observed prior to crystallization (Braggs peaks appear only after the start of crystallization at  $T \geq 625$  K). Following Chen,<sup>19</sup> Schluckebier and Predel<sup>11</sup> interpreted this double  $T_g$  effect and the first exothermic peak in terms of a phase separation into zones of two glasses with different compositions and different  $T_g$ 's. In Fig. 1, however, no change in the scattering intensity  $I(Q, T)$  is observed as the sample undergoes the exothermic phenomenon responsible for the first peak on the thermogram. The background intensity is too low to appear on the scale of this figure. Figure 3 does show a sharp increase in  $I(Q, T)$  with the onset of crystallization at  $T \approx 260$  K and in agreement with the second peak of the DSC thermogram.

#### B. The isochronal heating of amorphous $\text{Cu}_{50}\text{Zr}_{50}$

Figure 2 shows the x-ray scattering intensity  $I(Q, T)$  versus  $Q$  for different temperatures during heating of an amorphous  $\text{Cu}_{50}\text{Zr}_{50}$  tape at 0.05 K/s or 3 K/min. Each curve or "frame" corresponds to photon counts during 360 sec or 6 min over a temperature range  $\Delta T = 9$  K centered about the indicated value. The background intensity  $I_0$  of the furnace without the sample, normalized for the same count of incident photons [see Eq. (1)] is shown below the first curve or frame corresponding to  $T = 578$

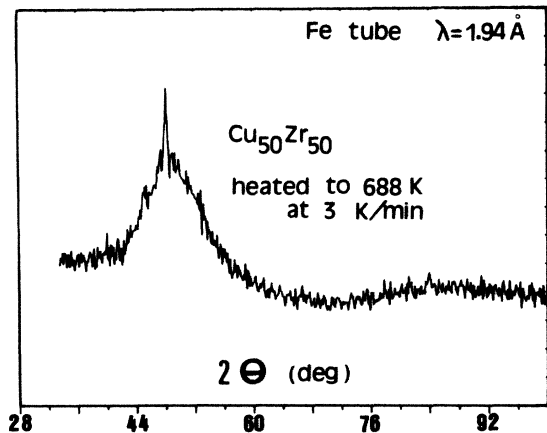


FIG. 4. Bragg peak emerging in diffraction pattern of amorphous  $\text{Cu}_{50}\text{Zr}_{50}$  after heating up to 688 K at 3 K/min. This onset of crystallization corresponds to the sharp increase in SAXS of Fig. 6 near 690 K.

K and can be seen to be small compared to the SAXS from the sample at low  $Q$ . No change in the SAXS from the sample  $I(Q, T)$  is observed between  $T=300$  and 668 K, which includes the range near  $T \approx 623$  K where Schultz *et al.*<sup>10</sup> have reported clear increases in the resistivity of amorphous  $\text{Cu}_{50}\text{Zr}_{50}$  which they attribute to a phase separation. Although they obtained the increase after longer annealing times, a similar phenomenon should have occurred at a few degrees higher temperature during our isochronal heating. Figure 3 shows SAXS measurements in amorphous  $\text{Cu}_{50}\text{Zr}_{50}$  heated in the same manner but up to higher temperature  $670 \leq T \leq 770$  K, which includes the crystallization stage ( $T \approx 700$  K) with a heating rate of 0.05 K/s (3 K/min). Here an increase in  $I(Q, T)$  is observed in two stages with a sharp rise between the two stages around  $T \approx 700$  K. This sharp rise is due to the onset of crystallization as observed in DSC measurements (for details of precision DSC measurements on this alloy, see, for example, Harmelin *et al.*<sup>20</sup>). Thermograms for amorphous  $\text{Cu}_{50}\text{Zr}_{50}$  obtained at heating rate  $dT/dt = 80$  K/min (1.33 K/s) show the onset of crystallization  $T_{\text{cryst}}$  at  $T = 720$  K. Now  $T_{\text{cryst}}$  is higher, the higher the heating rate  $dT/dt$ , and follows approximately  $\Delta T_{\text{cryst}} \approx 10 \Delta \ln(dT/dt)$ ,<sup>21</sup> so that in the SAXS experiment of Fig. 3 with  $dT/dt = 3$  K/min, the onset temperature,  $T_{\text{cryst}}$  of crystallization is near  $T = 690$  K and thus accounts for most, if not all the increase in  $I(Q, T)$  at  $T \approx 690$  K. Figure 4 shows x-ray diffraction in a sample heated at 3 K/min up to 690 K and it can be seen that the early stage of crystallization has started here thus resulting in the  $I(Q, T)$  increase at  $T \leq 690$  in this experiment.

#### IV. DISCUSSION

Our dynamic high-intensity SAXS measurements during isochronal heating of amorphous Cu-Zr and

$\text{Pd}_{46}\text{Ni}_{36}\text{P}_{18}$  foils failed to confirm the development of compositional heterogeneities in the temperature ranges that others have claimed occurrence of phase separation phenomena in these glasses.

The following questions, however, should be dealt with before drawing conclusions. In case of the development of compositional fluctuations (a) what is the range of amplitudes of such fluctuations (or variations in corresponding electron density  $\rho$  ( $e^-/\text{\AA}^3$ ) that would have been detected? and (b) what range of scale or spacial distribution of fluctuations would have been detected under the conditions of our SAXS experiment?

The determination of electron density variations corresponding to a scattering intensity from an unknown phase distribution requires the knowledge of the absolute value of the incident beam intensity  $I_0$ . We do not dispose of  $I_0$  but to answer question (a), we can estimate the local electron density variations  $\Delta\rho$  by comparison of their SAXS intensities  $I(Q)$  with the strong SAXS obtained from the crystallized states for which  $\Delta\rho$  is known to a good approximation.

The scattering intensity  $I(Q)$  is directly proportional to  $\Delta\rho^2 V(1-V)$  for  $\Delta\rho = \rho_p - \rho_m$  where  $V$  is the volume fraction of particles with  $\rho = \rho_p$  in a matrix with electron density  $\rho = \rho_m$ . For an alloy with volume per atom  $V_p$  and  $V_m$  ( $\text{\AA}^3$ ) in the particles and the matrix, respectively,  $\Delta\rho$  is given by

$$\Delta\rho^2 = (\rho_p - \rho_m)^2 = \left[ \sum_i X_i^p f_i / V_p - \sum_i X_i^m f_i / V_m \right]^2, \quad (2)$$

where  $X_i^p$  and  $X_i^m$  are the atomic fractions of elements  $i$  in the particles and the matrix and  $f_i$  is the number of electrons of the  $i$ th element.  $V_p$  and  $V_m$  can be calculated from experimental alloy mass density  $d$ , measured for different concentrations using  $V_j = \sum_i m_i^j X_i^j / d^j$  where  $m_i$  are the masses of each of the alloy's constituent atoms. For a given volume fraction  $V$  of particles with  $e^-$  density  $\rho_p$  in a matrix of  $e^-$  density  $\rho_m$ , the integrated intensity is related to  $\Delta\rho$  by

$$\int_0^\infty Q^2 I(Q) dQ = 2\pi^2 \Delta\rho^2 V(1-V) \quad (3)$$

whatever the particle-size distribution.<sup>22</sup> Figure 5 shows  $I(Q, T)$  for  $\text{Pd}_{46}\text{Ni}_{36}\text{P}_{18}$  at 676 and 604 K after the background correction of Eq. (1). The curve at  $T = 604$  K corresponds to  $I(Q, T)$  for any temperature  $T \leq 610$  K, a range which includes the first exothermic peak of the DSC thermogram (hitherto attributed to phase separation) and the *as-quenched* state.  $I(Q, 676 \text{ K})$  corresponds to the fully crystallized sample (see Fig. 1). Also drawn as an example, is a hypothetical curve (dashed line) hereafter referred to as  $I(Q, T^*)$  which corresponds to the addition of 10% of the  $I$  increase upon crystallization to  $I(Q, T)$  at  $T = 604$  K. From an experimental point of view, such an increase occurring in the range  $520 \leq T \leq 610$  K of the first DSC exotherm would have been easily measured.

Since we are testing the hypothesis of a phase separation during heating of an *as-quenched* homogeneous phase, we may deduce the temperature independent intensity (the 604 K curve) which is probably due to

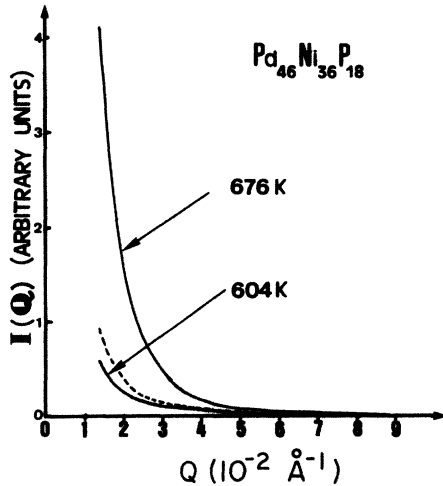


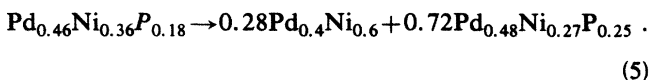
FIG. 5. SAXS in amorphous  $\text{Pd}_{46}\text{Ni}_{36}\text{P}_{18}$  at 676 K (fully crystallized) and at 604 K (prior to crystallization) after correction for background intensity (see text for details).

quenched-in defects and external surfaces [we will return to this  $I(Q)$  level of the *as*-quenched state later]. After this subtraction we obtain for the dashed curve and the crystallized state

$$\begin{aligned} & \int_0^\infty Q^2 \cdot I(Q, T^*) dQ / \int_0^\infty Q^2 \cdot I_{\text{cryst}}(Q, 676 \text{ K}) dQ \\ & = 0.1 = \Delta\rho^2 \cdot V^*(1-V^*) / \Delta\rho_{\text{cryst}}^2 V(1-V) \\ & = (\Delta\rho / \Delta\rho_{\text{cryst}})^2 \end{aligned} \quad (\text{spinodal decomposition}) . \quad (4)$$

To obtain the last equality of Eq. (4), we have supposed that the total volume fractions concerned by the eventual phase separation stage and the crystallization stage that follows are the same. This is reasonable because the amorphous chemically heterogeneous zones are expected to occur by spinodal decomposition rather than nucleation and growth and the crystalline phases will then form first in the zones corresponding to their compositions. It should be noted, however, that differences in size distribution (grain or zone size do not modify the integrated intensities).<sup>22</sup>

Figure 6 shows electron density  $\rho$  as a function of composition in amorphous and crystalline Pd-Ni-P alloys calculated using Eq. (2) and the density data collected in.<sup>23</sup> Amorphous  $\text{Pd}_{46}\text{Ni}_{36}\text{P}_{18}$  alloy of near eutectic composition crystallizes into a nickel-rich fcc solid solution and a palladium-rich  $(\text{PdNi})_3\text{P}$  intermetallic phase. Energy dispersive x-ray microanalysis indicates that the Ni/Pd ratio is about  $\frac{3}{2}$  in the fcc phase.<sup>24,25</sup> It follows that the crystallization products consist of



The electron-density difference between the two crystallization products is therefore  $\Delta\rho_{\text{cryst}} \approx 0.28 e^-/\text{\AA}^3$

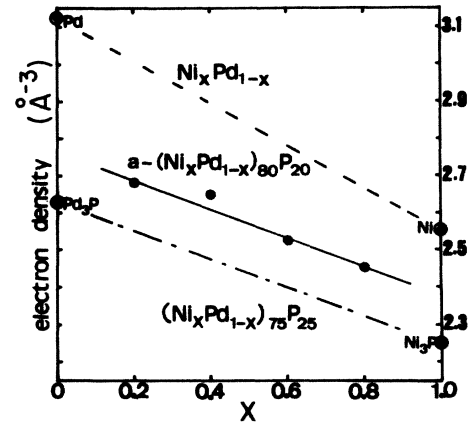


FIG. 6. Electron density  $\rho$  ( $e^-/\text{\AA}^3$ ) for various amorphous ( $\bullet$ ) and crystalline ( $\circ$ ) compositions of the Pd-Ni-P alloys calculated from available density data as collected by Gaskell (Ref. 23) using Eq. (2).

from Fig. 6. According to Eq. (4), an intensity increase such as that of the dashed line of Fig. 5 would therefore correspond to  $\Delta\rho \approx 0.28 \sqrt{0.1} \approx 0.09 e^-/\text{\AA}^3$  which fixes roughly the lower limit of electron-density fluctuations that we would have easily measured in this alloy. The phosphorous contrast  $\Delta C_p \approx 25\%$  between the crystallization products. The above discussion suggests that we would have clearly detected fluctuations in *P* content of  $\approx 5$  at. %.

Figure 7 shows  $I(Q, T)$  for  $\text{Cu}_{0.5}\text{Zr}_{0.5}$  at 770 and 670 K after background corrections [Eq. (1)].  $I(Q, 770 \text{ K})$  corresponds to the crystallized state while  $I(Q, 670 \text{ K})$  corresponds to the scattering at  $T \leq 670 \text{ K}$  before the rise observed in Fig. 4. As in Fig. 5 for the Pd-Ni-P glass, we have also drawn a hypothetical curve (dashed line) here-

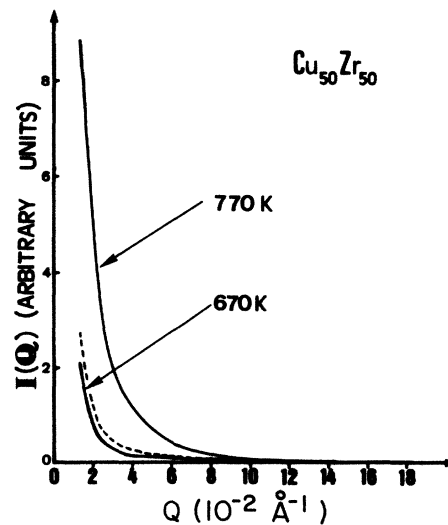


FIG. 7. SAXS in amorphous  $\text{Cu}_{0.5}\text{Zr}_{0.5}$  at 770 K (crystallized) and 670 K (prior to crystallization) after correction for background intensity (see text for details).

after referred to as  $I(Q, T^*)$  corresponding to the addition of 10% of the difference between  $I(Q, 770 \text{ K})$  and  $I(Q, 670 \text{ K})$  to the latter. Again such an increase is in the range that would have been easily detected in our experiment had it occurred in the  $T$  range of presumed phase separation. Using Eq. (4), we can consider  $I(Q, T^*)$  to correspond to an electron-density increase  $\Delta\rho = \Delta\rho_{\text{cryst}}\sqrt{0.1}$  where  $\Delta\rho_{\text{cryst}}$  depends on the crystallization products of the reaction.<sup>26</sup>

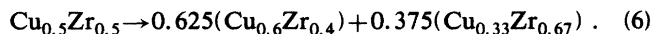


Figure 8 shows electron density  $\rho$  versus copper content in some amorphous and crystalline compositions in the Cu-Zr alloy system calculated using Eq. (2) and the mass densities reported in Ref. 27. It can be seen that  $\Delta\rho_{\text{cryst}} = 0.2 e^-/\text{\AA}^3$  for the products of the reaction of Eq. (6). Equation (4) would indicate that the dashed line corresponds to electron-density variations  $\Delta\rho = \sqrt{0.1}\Delta\rho_{\text{cryst}} = 0.07 e^-/\text{\AA}^3$  and comparison with Fig. 8 would indicate that our measurements would have easily detected concentration fluctuations of the order of  $\Delta C = 10 \text{ at. \%}$  in Cu or Zr (this corresponds to variations of  $\approx 5 \text{ at. \%}$  from the global composition).

We wish to point out that the scattering intensities  $I(Q)$  of the *as*-quenched amorphous foils and in particular their  $Q$  dependence are quite similar to those of elemental pure foils (such as that of pure Cu) tested under the same conditions. The *as*-quenched signal can thus be attributed to density defects (such as dislocations, quasi-dislocations, and voids) and to the external foil surfaces. The slightly faster increase of  $I(Q)$  with decreasing  $Q$  in the case of amorphous CuZr foils (which are initially much thinner) can be attributed to a faster quench rate used in their preparation and to a stronger tendency towards oxidation after thinning. We can therefore suppose that our *as*-quenched glasses are homogeneous to within the limits of detection of our experiment and that we can deduct the intensity  $I(Q)$  in the *as*-quenched state from the subsequent increase during heating as we have done in the above discussion [see Eq. (4)]. However, we

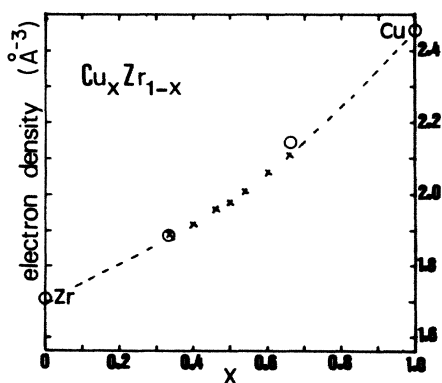


FIG. 8. Electron density  $\rho$  ( $e^-/\text{\AA}^3$ ) for amorphous ( $\times$ ) and crystalline ( $\circ$ ) Cu-Zr alloys calculated from the density data in (27) using Eq. (2).

also checked the consequence of attributing the *as*-quenched  $I(Q)$  to some high-temperature phase separation occurring in the liquid alloy during the quench (at  $T > T_{\text{cryst}}$ ). Numerical integration of Eq. (3) with truncation at the highest  $Q$  value of  $0.26 \text{ \AA}^{-1}$  and using estimated  $I(0)$  obtained from the extrapolation of the slope of Guinier plots to  $Q = 0$  for the sets of curves presented in Figs. 5 and 7 indicated that  $I(Q)$  increases of the order of those of the dashed lines would correspond to further phase separation and development of concentration fluctuations during heating of the order of 2 at. %.

Question (b) concerning the scale of any composition fluctuations that would be detected in our experiment can be addressed as follows: the scattering level  $I(0)$  at  $Q = 0$  from any set of particles depends on their electron-density contrast and is equal to the integrated intensity of Eq. (3) times the particles' volume.<sup>22</sup>  $I(Q)$  then drops off from its  $I(0)$  value with increasing  $Q$  more or less rapidly depending on the particles' shape and distribution and in general, the smaller the particles, the slower is the decrease with increasing  $Q$ . For the case of spherical particles of radius  $R$ ,  $I(Q)$  is given by<sup>22</sup>

$$I(Q) = I(0) \exp(-R^2 Q^2 / 3) \quad (7)$$

This equation holds for  $Q < 1/R$  and is a good approximation for spheres of radii up to  $Q < 2/R$ . Since  $I(0)$  is not experimentally observable,  $I(Q)$  is best measured at the lowest possible  $Q$  values but at very low wave vectors ( $Q < 10^{-2} \text{ \AA}^{-1}$ ) surface scattering independent of Eq. (7) dominates the SAXS (Refs. 28 and 29). In our experiment the lowest wave-vector modulus  $Q = 1.4 \times 10^{-2} \text{ \AA}^{-1}$ . At this  $Q$  value, particles of appropriate electron density contrast and of radii  $R < 2/Q \approx 140 \text{ \AA}$  emerging during the isochronal annealing prior to crystallization should produce significant scattering intensity increase but no such increases were observed in the temperature range of interest. Furthermore, no Guinier fit [linear zone on  $\ln I(Q)$  versus  $Q^2$ ] was obtained in any  $Q$  range.

When such compositional heterogeneities with interparticle spacing  $L$  appear, an interference peak is expected on the  $I(Q)$  curve near  $Q = 2\pi/L$  (see Ref. 30). The  $Q$  range of our experiment was  $0.014 \leq Q \leq 0.258 \text{ \AA}^{-1}$  but in the range  $Q > 0.1 \text{ \AA}^{-1}$  the intensity is too low to be credible. This indicates that interference peaks due to interparticle spacing  $60 \leq L \leq 450 \text{ \AA}$  would have been detected. Our experiments were thus appropriate for the detection of the emergence of chemical heterogeneities of dimensions  $2R \leq 200 \text{ \AA}$  spaced between 60 to 450  $\text{\AA}$  from each other provided that their atomic compositions differed by 5 to 10 at. % from their surroundings but no such concentration fluctuations were detected. Our TEM and scanning transmission electron microscopy (STEM) observations on Pd-Ni-P confirm that no such zones with  $R \approx 10 \text{ \AA}$  exist in this amorphous alloy prior to the onset of crystallization.<sup>25</sup> In CuZr, compositional fluctuations with  $R \approx 150 \text{ \AA}$  could have remained undetected in our experiment but this can only apply to the *as*-quenched alloy since the growth of any such zones during our experiment would have been signaled by increasing  $I(Q)$  before they grow to such dimensions. (It should be noted that the  $Q$  dependence of the law of Guinier and the oc-

currence of interference peaks as discussed here do not apply to the crystallization of amorphous alloys which under usual heating conditions proceeds from the sample surfaces towards the inside or by growth of preexisting crystal nuclei; see, for example, Refs. 31 and 32.)

Very recently, Deng and Argon<sup>33</sup> have presented TEM results on annealed amorphous  $\text{Cu}_{59}\text{Zr}_{41}$  clearly indicating occurrence of phase separation and double halos in the electron SAD patterns even in the *as-received* state of the amorphous ribbons. This recalls the observations of Barbee *et al.*<sup>34</sup> showing x-ray and electron diffraction double halos in vapor deposited  $\text{Cu}_{50}\text{Zr}_{50}$  amorphous foils. We have seen no such evidence by x-ray diffraction in unthinned compositions of  $\text{Cu}_{50}\text{Zr}_{50}$  and  $\text{Cu}_{64}\text{Zr}_{36}$  which we prepared by quenching from the liquid state under helium gas, compositions which envelop the composition of Deng and Argon.<sup>33</sup> Also x-ray diffraction experiments by Chen *et al.*<sup>35</sup> on amorphous  $\text{Cu}_{55}\text{Zr}_{45}$  before and after annealing showed a slight sharpening of the single amorphous halo while Schultz *et al.*<sup>10</sup> reported a widening of the amorphous halo in  $\text{Cu}_{50}\text{Zr}_{50}$  after annealing. Significant differences thus appear between different Cu-Zr samples of comparable compositions and may be due to differences in the preparation procedure. Furthermore, given the probable high oxygen content in Zr-based alloys, the presence or formation of oxide

glasses during preparation or post-quench treatment may also be involved.<sup>36</sup>

## V. CONCLUSIONS

We have used an original combination of experimental improvements to achieve the precision required to obtain real time SAXS variation as a function of time and temperature during post-quench thermal treatment of metallic glasses. These include *in situ* heat treatments by Joule self-heating of the samples and the use of high-intensity x-ray beam from a powerful synchrotron as well as the use of regular wide amorphous tapes prepared by planar flow casting.

We found no evidence of phase separation during heating in glassy  $\text{Pd}_{46}\text{Ni}_{36}\text{P}_{18}$  and  $\text{Cu}_{50}\text{Zr}_{50}$  alloys prior to crystallization. The results exclude the occurrence of any such zones with radii  $10 \lesssim R \lesssim 100 \text{ \AA}$  with deviations of more than 5 at. % from the global alloy composition.

## ACKNOWLEDGMENTS

This work was supported by the Centre National de la Recherche Scientifique (CNRS) of France and the Japanese Society for the Promotion of Science (JSPS) of Japan. Laboratoire de Thermodynamique Physico-Chimie is Laboratoire No. 29 associé au CNRS.

- <sup>1</sup>C. O. Kim and W. C. Johnson, *Phys. Rev. B* **23**, 143 (1981).
- <sup>2</sup>A. R. Yavari, *International J. Rapid Solidification* **9**, 47 (1986); *Acta Metall.* (to be published).
- <sup>3</sup>A. R. Yavari, S. Nishitani, P. Desré, and P. Chieux, *Z. Phys. Chem. Neue Folge* **157**, 103 (1988).
- <sup>4</sup>C. P. Chou and D. Turnbull, *J. Non-Cryst. Solids* **17**, 169 (1975).
- <sup>5</sup>J. L. Walter, D. G. Legrand, and F. E. Luborsky, *Mater. Sci. Eng.* **29**, 161 (1977).
- <sup>6</sup>J. L. Walter, F. Bacon, and F. E. Luborsky, *Mater. Sci. Eng.* **24**, 239 (1976).
- <sup>7</sup>A. R. Yavari, D. Bijaoui, M. C. Bellissent, P. Chieux, and M. Harmelin, in *Magnetic Properties of Amorphous Metals*, edited by A. Hernando (Elsevier, New York, 1987), pp. 336–339.
- <sup>8</sup>A. R. Yavari (unpublished).
- <sup>9</sup>D. Bijaoui, Doctoral thesis, Institut National Polytechnique de Grenoble, 1987.
- <sup>10</sup>R. Schultz, K. Samwer, and W. L. Johnson, *J. Non-Cryst. Solids* **61-62**, 997 (1984).
- <sup>11</sup>G. Schluckebier and B. Predel, *Z. Metallkd.* **74**, 569 (1983).
- <sup>12</sup>J. Piller and P. Haasen, *Acta Metall.* **30**, 1 (1982).
- <sup>13</sup>M. Murakami, O. Kawano, Y. Murakami, and Morinaga, *Acta Metall.* **17**, 1517 (1969).
- <sup>14</sup>K. Osamura, K. Okuda, H. Hashinzume, and Y. Amemia, *Acta Metall.* **33**, 2199 (1985).
- <sup>15</sup>Narasimhan, U. S. Patent No. 4142571 (1979).
- <sup>16</sup>A. R. Yavari and P. Desré, in *Magnetic Properties of Amorphous Metals*, edited by A. Hernando (North-Holland, Amsterdam, 1987), pp. 6–14.
- <sup>17</sup>A. R. Yavari, *J. Mater. Res.* **1**, 746 (1986).
- <sup>18</sup>A. R. Yavari and K. Osamura, *Rev. Sci. Instrum.* **58**, 1177 (1987).
- <sup>19</sup>H. S. Chen, *Mater. Sci. Eng.* **23**, 151 (1976).
- <sup>20</sup>M. Harmelin, A. Naudon, J. M. Frigerio, and J. Rivory, *Rapidly Quenched Metals (RQ5)*, edited by S. Steeb and H. Warlimont, (Elsevier, New York, 1985) pp. 659–662.
- <sup>21</sup>H. S. Chen, *Rapidly Quenched Metals (RQ4)*, edited by T. Masumoto and K. Suzuki (Japan Institute of Science, Japan, 1982) Vol. I, p. 445–500.
- <sup>22</sup>A. Guinier and F. Fournet, *Small Angle Scattering of X-Rays* (Wiley, New York, 1955).
- <sup>23</sup>P. H. Gaskell, *Acta Metall.* **29**, 1203 (1981).
- <sup>24</sup>P. E. Donovan, P. V. Evans, and A. L. Greer, *J. Mater. Sci. Lett.* **5**, 951 (1986).
- <sup>25</sup>A. R. Yavari and S. Hamar-Thibault (unpublished).
- <sup>26</sup>E. Kneller, Y. Khan, and U. Gorres, *Z. Metallke.* **77**, 43 (1986).
- <sup>27</sup>Y. Calvayrac, J. P. Chevalier, M. Harmelin, A. Quivy, and J. Bigot, *Philos. Mag. B* **48**, 323 (1983).
- <sup>28</sup>W. H. Robinson and R. Smoluchowski, *J. Appl. Phys.* **27**, 657 (1956).
- <sup>29</sup>A. R. Yavari, P. Desré and P. Chieux, in *Atomic Transport and Defects in Metals by Neutron Scattering*, edited by C. Janot *et al.*, (Springer-Verlag, city, 1986) pp. 42–49.
- <sup>30</sup>V. Gerold, *J. Appl. Cryst.* **11**, 376 (1978).
- <sup>31</sup>U. Koster and U. Herold, in *Glassy Metals I*, of Vol. 46, *Topics in Applied Physics*, edited by H. J. Guntherodt and H. Beck (Springer-Verlag, city, 1981) pp. 245–259.
- <sup>32</sup>K. F. Kelton and F. Spaepen, *Acta Metall.* **33**, 455 (1985).
- <sup>33</sup>D. Deng and A. S. Argon, *Acta Metall.* **34**, 3011 (1986).
- <sup>34</sup>T. W. Barbee, R. G. Walrmsley, A. Marshall, D. L. Keith, and D. A. Stevenson, *J. Appl. Phys. Lett.* **38**, 132 (1981).
- <sup>35</sup>H. S. Chen, K. T. Aust, and Y. Waseda, *J. Mater. Sci. Lett.* **2**, 153 (1983).
- <sup>36</sup>J. P. Chevalier, Y. Calvayrac, A. Quivy, M. Harmelin, and J. Bigot, *Acta Metall.* **31**, 465 (1983).